UDK 539.3

S.M. Vereshchaka, professor,
Emad Toma Karash, postgraduate,
Sumy State University

DELAMINATION STRESSES IN THIN-WALL STRUCTURES OF COMPOSITE MATERIALS

С.М. Верещака, Імад Тома Каракаш. **Напруги розшарування в тонкостійних структурах композиційних матеріалів.** Класична теорія анізотропної пружності застосована для розробки багатошарової теорії за допомогою програми MathCAD 14 з метою визначення полів напруження і деформації, що виникають у багатошаровому півкруглому кривому стержні з композитного матеріалу, підданого кінцевим силам. Спочатку визначені радіальне положення, інтенсивність напруги розшарування, а потім проводилося порівняння з результатами проведених експериментів, теорією анізотропного суцільного середовища і методом ANSYS. Багатошарова теорія дає можливість більш точного визначення положення і інтенсивності напруги розшарування, а також зсувів, порівняно з результатами, отриманими за допомогою теорії анізотропного суцільного середовища. Експериментальні результати схожі з результатами багатошарової теорії.

Ключові слова: багатошарова теорія, розшарування, теорія анізотропного суцільного середовища, напівкруглий шаруватий матеріал.

С.М. Верещака, Імад Тома Каракаш. **Напряжения расслоения в тонкостенных структурах композитных материалов** Классическая теория анизотропной упругости применена для разработки многослойной теории при помощи программы MathCAD 14 с целью определения полей напряжения и деформации, возникающих в многослойном полукруглом кривом стержне из композитного материала, подверженного конечным силам. Вначале определены радиальное положение, интенсивность напряжения расслоения, а затем производилось сравнение с результатами проведенных экспериментов, теорией анизотропной сплошной среды и методом ANSYS. Многослойная теория дает возможность более точного определения положения и интенсивности напряжения расслоения, а также смещений, по сравнению с результатами, полученными при помощи теории анизотропной сплошной среды. Экспериментальные результаты схожи с результатами многослойной теории.

Ключевые слова: многослойная теория, расслоение, теория анизотропной сплошной среды, полукруглый слоистый материал.

S.M. Vereshchaka, Emad Toma Karash. **Delamination stresses in thin-wall structures of composite materials.** The classical anisotropic elasticity theory was used to construct multilayer theory for the calculation of the stress and deformation fields induced in the multilayered composite semicircular curved bar subjected to end forces and end moments by using program MathCAD 14. The radial location and intensity of the open mode delamination stress were calculated and were compared with the results obtained from the anisotropic continuum theory and ANSYS method. The multilayer theory gave more accurate prediction of the location and intensity of the open mode delamination stress, and of the offsets, than those calculated from the anisotropic continuum theory and practical results were identical with the results of multilayer theory

Keywords: multilayer theory, delamination, anisotropic continuum theory, semicircular laminated material.

1. Introduction

Composites laminates are widely used in both civil and military aircraft structures and gases cylinders leading to weight saving. However, study of the behaviour of such materials has shown that they are more damage sensitive than metallic material especially to delamination due to edge effect or low velocity impact [1]. In order to improve the performance of composite structures, advances must be made in the prediction of delamination growth and the evaluation of residual strength. The aim of this paper is to extend a delamination model valid for the plate in small displacement [2] or large displacement [3] to the case of curved structures as shells. Two kinds of approach are commonly used to study delamination growth, (i) the damage mechanics approach in which the interface enclosing the delamination is modelled by a damageable material Delamination is obtained when the damage variable reaches its maximum value [4...6] and (ii) the fracture mechanics approach which the present

work is part. In such an approach, the de1amination characteristic is the stress intensity factors [7, 8] and more generally the local energy release rate computed using either the virtual closure technique [8]. In most engineering applications, laminated composite structures have certain curvatures (for example, curved panels and curved beams). If the curved composite structure is .subjected to bending that tends to flatten the composite structure, tensile stresses can be generated in the thickness direction of the composites. Also, shear stresses could be induced if the bending is not a "pure" bending. Under normal operations, if the above type of bending occurs cyclically, open-mode delaminations or shear-mode delaminations could nucleate at the sites of peak interlaminar tensile stresses or at the sites of peak interlaminar shear stresses. Continuation of these bending cycling will cause the delamination zones to grow in size and ultimately cause the composite structures to lose their structural integrity (loss of stiffness and strength) due to excessive delaminations.

Fig. 1. Laminated composite curved-bar coupon for delamination study

The type of delamination failure (open mode or shear mode) depends on which type of interlaminar strength (tensile or shear) is reached first. The MATH-CAT 14 method were used to perform similar delamination analysis of the multilayered semicircular composite curved bar subjected to end forces and end moments. The resulting predictions of locations and intensities of peak radial stresses are compared with the results of the anisotropic continuum theory presented in reference [9].

2. Composite curved bar

Figure 1 shows the geometry of the composite curved bar (C-coupon) for de1amination fatigue tests of composite materials. Because finite areas are needed for the load application points. Both ends of the curved bar must be extended slightly. Thus, the C-coupon consists of a semicircular curved region with straight regions at both ends. Under the application of end forces P. the loading axis will have certain offset e from the vertical diameter of the semicircle. Thus, the loading condition on the C-coupon is the summation of the following two loading conditions (see fig. 2): (1) end forces-P at the ends of the semicircle and (2) end moment $M = Pe$ at the ends of the semicircle. Because the interface between 0° and 90° composite plies has the highest Poisson's ratio mismatch in laying up the composite plies for fabricating the C-coupon, it is desirable to place the 90° or angle plies at the peak radial stress point to ensure that the del8mination will nucleate at that point Because of this demand. The precise location of the peak radial stress point must be known. The following sections will show how to determine the intensities and radial locations of peak radial stresses in the semicircular composite curved bar.
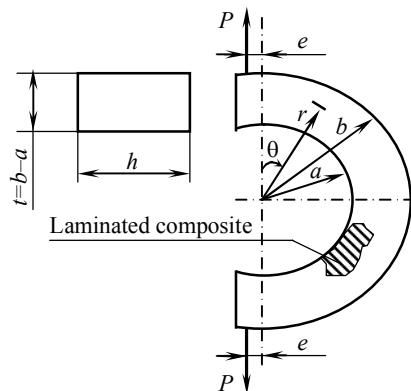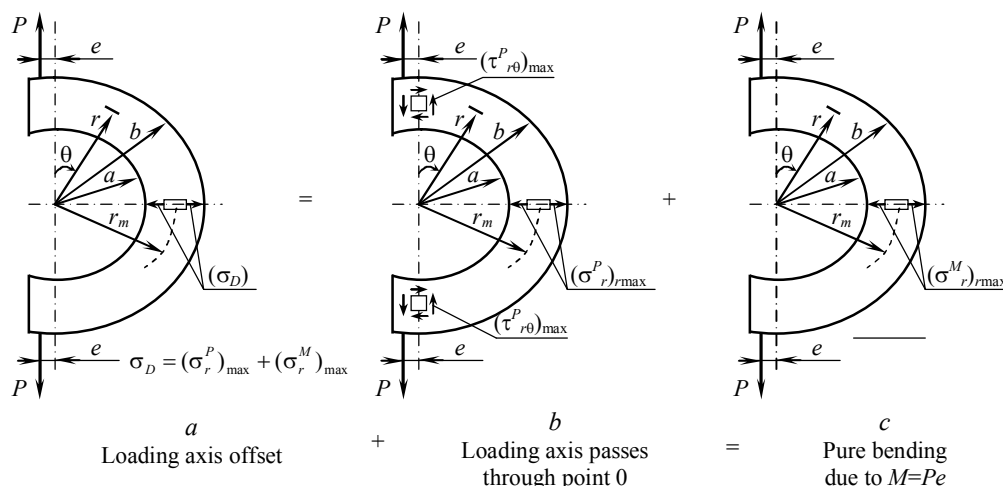

Fig. 2. Bending of curved bar by forces at its ends. Loading axis has offset e
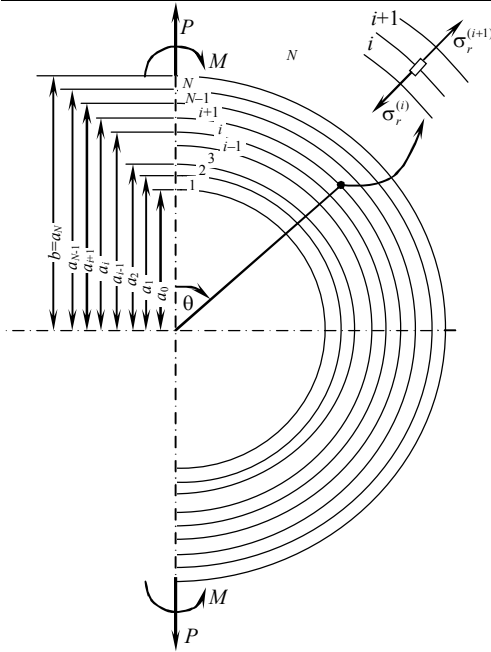
Fig. 3. Bending of laminated anisotropic semicircular curved bar by end forces and moments

3. Anisotropic continuum theory

For bending a linearly elastic continuous curved bar with cylindrical anisotropy. The Airy stress function F. written in cylindrical coordinate system takes on the following functional forms [5].

4. Multilayer trheory

Figure 3 shows the multilayer (*N*-layers), semicircular curved bar subjected to both end forces and end moments *M*. The stress field and displacement field in each layer *i* (*i*=1, 2, …, *N*) for each loading case may be obtained from the results given in section 3.

Delamination stress and their locations

At exactly which layer the value of σ_r for each loading case will become maximum cannot be predicted until after all the unknown arbitrary constants $\{A_i, B_i, D_i\}$ or $\{B'_i, C'_i, D'_i\}$. Suppose $[(\sigma_r^p)_{max}$ or $(\sigma_r^M)_{max}]$, the maximum value of σ_r due to end forces *P* (or end moments *M*). Occurs in the i_{th} layer; then by using the extreme condition $\frac{\partial}{\partial r}\sigma_r = 0$.

The radial location $[r_m^p$ or r_m^M of $(\sigma_r^p)_{max}$ or $(\sigma_r^M)_{max}]$

5. Finite element approach

By using Ansys 10.0 finite element analysis software, a static failure analysis was performed on an element of a composite curved bar. First element type was defined with solid layered 46 Figure 4. Solid46 is a layered version of the 8-node structural solid element designed to model layered thick shells or solids. The element allows up to 250 different material layers. The element may also be stacked as an alternative approach. The element has three degrees of freedom at each node: translations in the nodal x, y, and z directions.

Real constant sets were defined for 54 layers, various orientation angle and each layers thickness was entered 0.37 mm . After material properties was defined, linear orthotropic material was chosen and the mechanical properties of graphite-epoxy composite material was added as *EX, EY, EZ, PRXY, PRYZ, PRXZ, GXY, GYZ* and *GXZ*. In order to calculate failure criteria, ultimate tensile strength, compressive strength and shear strength were entered both in fiber direction and in matrix direction. Then a volume block was modeled and material properties, real constant sets and element type were appointed to this volume. After that the model was meshed by using hexahedral sweeped elements.

6. Experiment details

Filament wound composite materials are used in commercial industries such as fuel tank, portable oxygen storage, and natural gas .The fibers used were semicircular bars . The bars typically 196 mm inner diameter , 200 mm outer diameter, 4 mm thickness, 48.3 mm width shown in figure 5 (*a*, *b*).

Results and Dissection

The anisotropic continuum theory and the multilayer theory presented respectively in section 3 and 4 will now be applied to the delamination analysis of composite semicircular curved bar under development has the following geometry and
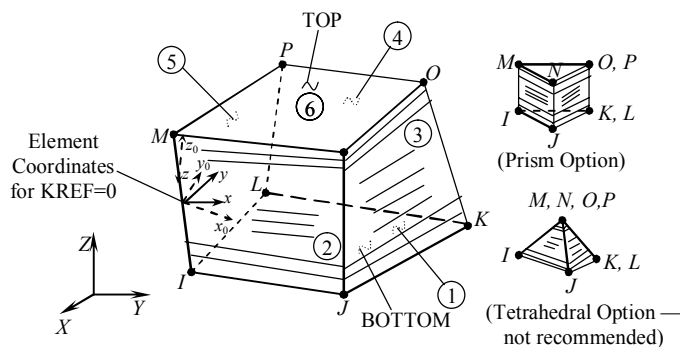

Fig. 4. SOLID46 Geometry

ply properties [inner radius (a = 100 mm), outer radius (b = 11.998 mm), loading axis offset (e = 40 mm), width (h = 25.4 mm), ply thickness(δ = 0,16 mm), (ψ_1 = 0,55), (ψ_3 = 0,15 ψ_1) where ψ_1 and ψ_3 — the relative volume content reinforcement layer in the direction of axis (1) and (3), E_L = 172369 MPa, E_T = 8274 MPa, G_{LT} = 4137 MPa, υ_{LT} = 0.33, υ_{TL} = 0,3. The semicircular curved bar has 54 composite plies having the stacking:$[0_{25}^\circ \,/ +15 \,/ -15 \,/ -15 \,/ +15 \,/ 0_{25}^\circ]$.

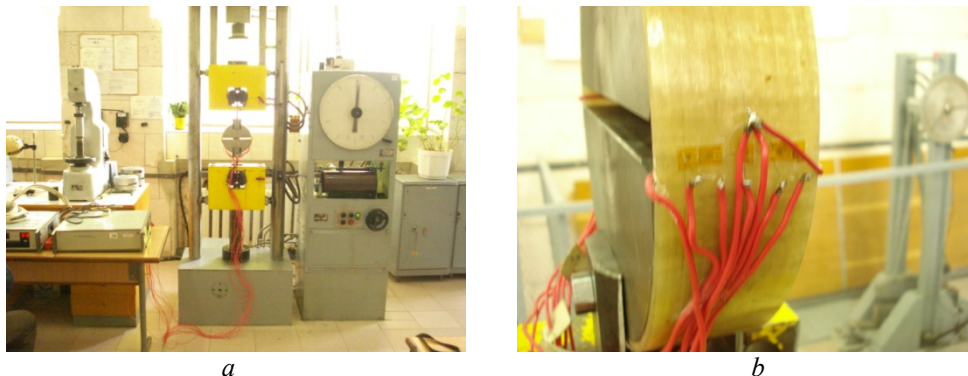*a*   *b*

Fig. 5 (a, b). Shown the bars, strain gauges and instruments were used in experiment

Equivalent continuum

In order to apply the anisotropic continuum theory, the laminated semicircular curved bar will be represented by an equivalent anisotropic continuum having the following effective material properties (Table 1).

Table 1

Effective material properties where applied anisotropic continuum theory

E_θ MPa	E_r MPa	E_z MPa	$G_{r\theta}$ MPa	G_{rz} MPa	$G_{\theta z}$ MPa	$\nu_{r\theta}$ MPa	ν_{rz} MPa	$\nu_{\theta z}$ MPa	β	k
124410	36705	48133	4838	5355	3470	0,042	0,317	0,312	5,462	1,841

Multilayer system

For the purpose of applying the multilayer theory to the semicircular curved bar. the extended linear regions at both ends will be neglected, and only the semicircular region subjected to two types of loadings (end forces P and end moments M. figure 2) will be considered. For simplification, inner region of 25 layers of the 0º plies will be represented by one layer of anisotropic continuum, and the center region of 4 layers of ±15º angle plies will be represented by another anisotropic continuum, outer region of 25 layers of the 0º plies will be represented by one layer of anisotropic continuum. Thus, the 54-layer composite will be represented by 3 layers of anisotropic continua (Table 2).

Table 2

Effective material properties where applied multilayer theory

Layers (1 and 3), 0˚ *plies*										
$E_\theta^{1,3}$ MPa	$E_r^{1,3}$ MPa	$E_z^{1,3}$ MPa	$G_{r\theta}^{1,3}$ MPa	$G_{rz}^{1,3}$ MPa	$G_{\theta z}^{1,3}$ MPa	$\nu_{r\theta}^{1,3}$ MPa	$\nu_{rz}^{1,3}$ MPa	$\nu_{\theta z}^{1,3}$ MPa	$\beta_{1,3}$	$k_{1,3}$
125653	36950	48122	9972	12737	8217	0,117	0,318	0,318	4,095	1,844
Layer (2), ±15˚ *plies*										
E_θ^2 MPa	E_r^2 MPa	E_z^2 MPa	$G_{r\theta}^2$ MPa	G_{rz}^2 MPa	$G_{\theta z}^2$ MPa	$\nu_{r\theta}^2$ MPa	ν_{rz}^2 MPa	$\nu_{\theta z}^2$ MPa	β_2	k_2
109338	34725	48377	17143	12433	8520	0,102	0,296	0,249	3,144	1,774

Figure 5 shows the distributions of σ_r^p in the $\theta = \pi/2$ plane for the case of end forces P calculated from different theories. The values of $\left(\sigma_r^p\right)_{max}$ and r_m^p calculated from different theories are indicated in the figure. The values of $\left(\sigma_r^p\right)_{max}$ calculated from different theories are quite close, except its location r_m. The multilayer theory method predicted close values of r_m^p. The $\left(\sigma_r^p\right)_{max}$ site predicted from the anisotropic continuum theory is located slightly closer to the middle surface than the $\left(\sigma_r^p\right)_{max}$ sites predicted from the multilayer theory. The $\left(\sigma_r^p\right)_{max}$ site for the isotropic material is closest to the middle surface and is always located between the middle surface and the $\left(\sigma_r^p\right)_{max}$ site predicted from the anisotropic continuum theory.

The distance between the sites of $\left(\sigma_r^p\right)_{max}$ predicted from the multilayer theory and the anisotropic continuum theory is

$$\left(r_m^p\right)_{\substack{\text{Anisotropic}\\\text{continuum}}} - \left(r_m^p\right)_{\text{Multilayer}} = 109,0734 - 108,8541 = 0,2193 \text{ mm}.$$

Which is 0,5927 times the single ply thickness of 0,37 mm.

Figure 6 shows the distributions of σ_r^M for the case of end moments M calculated from different theories. Unlike the previous case, the values of r_m^M and $\left(\sigma_r^M\right)_{max}$ calculated from different theories are quite close. Showing that the value of r_m^M is quite insensitive to the theory used. The multilayer theory predicted the shortest distance of r_m^M (that is, the $\left(\sigma_r^M\right)_{max}$ site is closest to the inner boundary of the curved bar). The site of $\left(\sigma_r^M\right)_{max}$ predicted from the anisotropic continuum theory always lies between the middle surface and the $\left(\sigma_r^M\right)_{max}$ site based on isotropic theory.

The distance between the sites of $\left(\sigma_r^M\right)_{max}$ predicted from the multilayer theory and the anisotropic continuum theory is given below

$$\left(r_m^M\right)_{\substack{\text{Anisotropic}\\\text{continuum}}} - \left(r_m^M\right)_{\text{Multilayer}} = 109,2337 - 109,2334 = 0,0003 \text{ mm}.$$

This is only 0,00081 times the single-ply thickness of 0,37 mm. and is therefore, Insignificant.
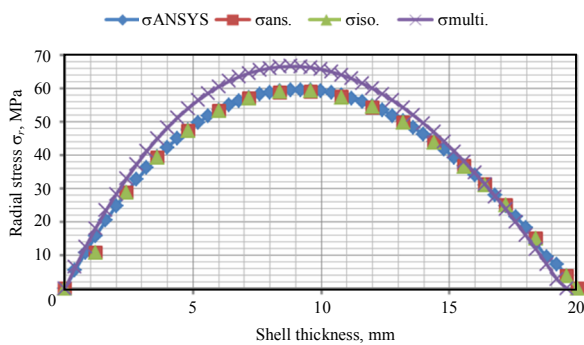

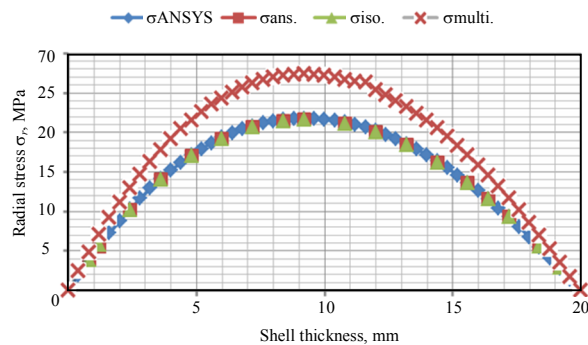*Fig. 6. Distribution of radial stress in (θ = π/2) plane, curved bar under end forces P*

Fig. 7. Distribution of radial stress in (θ = π/2) plane, curved bar under end moments M

Table 3 summarizes all the values of $\left(\sigma_r^p\right)_{max}$, r_m^p, $\left(\sigma_r^M\right)_{max}$, r_m^M calculated from different theories.

Table 3

Intensities and locations of delamination stresses in semicircular curved bar end force

Theory	End forces P			
	r_{max}^p, mm	$\left(\sigma_r^p\right)_{max}$, MPa	$\dfrac{h(b-a)}{P}\left(\sigma_r^p\right)_{max}$	$\dfrac{r_m^p - a}{b - a}$
Isotropic continuum	109,0736	59,08	1,4991	0,4541
Anisotropic continuum	109,0734	59,08	1,4991	0,4541
ANSYS	109,1938	59,6	1,5123	0,4601
Multilayer theory	108,8541	66,58	1,6895	0,4431
Experiment results	108,768	65,12	1,6543	0,4421

Table 4

Intensities and locations of delamination stresses in semicircular curved bar end bending moment

Theory	End forces M			
	r_{max}^M, mm	$\left(\sigma_r^M\right)_{max}$, MPa	$\dfrac{h.am.(b-a)}{M}\left(\sigma_r^M\right)_{max}$	$\dfrac{r_m^M - a}{b - a}$
Isotropic continuum	109,2333	21,6	1,5972	0,4621
Anisotropic continuum	109,2337	21,59	1,5067	0,4621
ANSYS	109,2016	21,8	1,521	0,4605
Multilayer theory	109,2234	27,37	1,9099	0,4616
Experiment results	109,123	26,12	1,8856	0,4342

Table 5

Shows the total stresses in equivalent semicircular curved bar.

Theory	$\sigma_r^D = \sigma_r^p + \sigma_r^M$	$\sigma_\theta^D = \sigma_\theta^p + \sigma_\theta^M$	$\tau_{r\theta}^D = \tau_{r\theta}^p + \tau_{r\theta}^M$
Isotropic continuum	80,68	715,98	59,8
Anisotropic continuum	80,67	542,55	59,6
ANSYS	81,4	545,4	59,7
Multilayer theory	93,95	546,34	66,7
Experiment results	91,24	545,33	64,3

The maximum tangential stress σ_θ is located at point ($r = a$, $\theta = 0^\circ$, 180°), but the maximum $\tau_{r\theta}$ is located at another point ($r = r_m$, $\theta = 90^\circ$).

Conclusions

The multilayer theory was developed for delamination analysis of a semicircular composite curved bar subjected to end forces and end moments. The difference between the radial locations of the delamination stress (maximum radial stress) predicted from the multilayer theory and from the anisotropic continuum theory was approximately 0,5927 times the ply thickness for the case of end forces and about 0,00081 times of the ply thickness for the case of end moments. The superposition method (namely, by summing up the two radial stresses induced in the semicircular curved bar subjected to end forces and end moments), used to construct the delamination stress in the C-coupon, gave reasonably accurate intensity of the delamination stress for the *C*-coupon. The finite element analysis of the C-coupon gave the radial location of the delamination stress in the C-coupon much closer to that

predicted from the multilayer theory than from the anisotropic continuum theory and practical results were identical with the results of multilayer theory.

References

1. Garg, A.C. Delamination — a Damage Mode in Composite Structures / A.C. Garg // Eng. Mech. Vol. 29/ — pp. 557 — 584.
2. Puck, B.A. Failure Analysis of FRP Laminates by means of Physically Based Phenomenological Models Comp / B.A. Puck, H. Schurmann. — Sci. and Tech., Vol. 58. — pp. 1045 — 1067.
3. Ko, W.L. Delamination Stresses in Semicircular Laminated Composite Bars / W.L. Ko // NASA T 4026, 1988.
4. Tolf, G. Stresses in a Curved Laminated Beam / G. Tolf // Fiber Science and Technology/ — 1983. — Vol. 19, #. 4. — pp. 243 — 267.
5. Leklmitskii, S.G. Anisotropic Plates / Gordon and Breach Science Publishers / S.G. Leklmitskii. — New York, 1968.
6. Whetstone, W.O. SPAR Structural Analysis System Reference Manual / W.O. Whetstone // System Level — 1978. — 13A. — Vol. I: Program Execution, NASA CR-15897o-1.
7. Puck, A. Festigkeitsanalyse von Faser-Matrix-Laminaten. Carl Hanser Verlag / A. Puck. — Munchen Wien, Germany, 1996.
8. Schuecker, C. D.H. Pahr, and H.E. Pettermann. Accounting for Residual Stresses in FEM Analysis of Laminated Structures Using the Puck Criterion for Three-Axial Stress States / C. Schuecker, D.H. Pahr, H.E. Pettermann // Comp. Sci. and Tech., 2006. — Vol. 66(13). — pp. 2054 — 2062.
9. Schuecker, C. Mechanism Based Modeling of Damage and Failure in Fiber Reinforced Polymer Laminates: thesis / C. Schuecker; Institute of Lightweight Design and Structural Biomechanics, Vienna University of Technology. — Vienna, Austria, 2005.